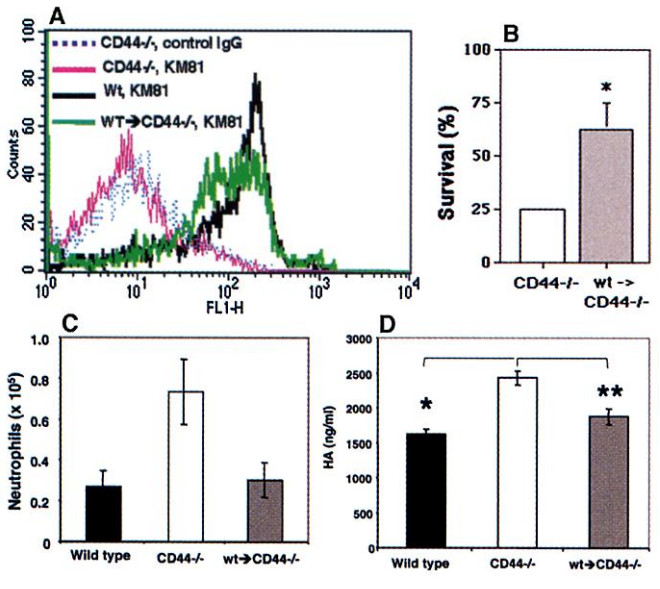

Fig. 4. Reversal of inflammatory phenotype by reconstituting CD44-deficient mice. (**A**) CD44$^+$ alveolar macrophages recruited to the lung after LPS challenge of CD44-deficient mice reconstituted with CD44$^+$ bone marrow (chimeric). (**B**) Survival at day 14 after bleomycin challenge in CD44-deficient and chimeric mice after reconstitution. Results are from two separate experiments with 10 mice in each group ($P < 0.05$). (**C**) Neutrophil clearance at day 14 after bleomycin in wild-type, CD44-deficient, and chimeric mice after reconstitution. Results are from 10 mice in each group ($P = 0.0269$). (**D**) HA clearance at day 14 after bleomycin in wild-type, CD44-deficient, and chimeric mice. Results are from 10 mice in each group. *$P = 0.002$ between wild type and CD44$^{-/-}$; **$P = 0.0097$ between CD44$^{-/-}$ and chimeric mice; and $P = 0.132$ between wild-type and chimeric mice.

with bone marrow from CD44$^+$ littermate controls (*22*). Successful reconstitution of CD44$^+$ alveolar macrophages and PMNs was demonstrated by fluorescence-activated cell sorting analysis of BAL cells from chimeric mice (Fig. 4A). Chimeric mice as well as reconstituted wild-type and CD44-deficient mice were challenged with intratracheal bleomycin and survival, inflammatory cell accumulation and HA content in BAL fluid were evaluated after 14 days. The survival defect and histologic changes in the lung tissue of the CD44-deficient animals after bleomycin treatment were significantly reversed by reconstitution with CD44$^+$ bone marrow (Fig. 4B). PMNs were cleared from the BAL fluid in both the wild-type and chimeric mice relative to the CD44-deficient mice (Fig. 4C). HA content was also reduced in the BAL fluid of the chimeric mice relative to the CD44-deficient mice (Fig. 4D). However, there was no significant difference in BAL fluid HA levels between wild type and chimeric mice suggesting that hematopoietic CD44 is the critical determinant of HA clearance after lung injury.

Previous studies have shown that CD44 is involved in recruiting T cells to inflammatory sites and regulates T cell–mediated endothelial injury (*23, 24*). Our results identify a previously unrecognized role for CD44 in resolving the inflammatory response following lung injury. CD44 deficiency leads to increased mortality from lung injury through unremitting inflammation characterized by accumulation of low-MW HA fragments, prolonged inflammatory gene expression, decreased clearance of apoptotic PMNs, and an impaired ability to generate active TGF-β_1. Reconstitution of CD44$^+$ alveolar cells partially reversed the phenotype demonstrating a requirement for CD44 in the successful resolution of the inflammatory response to tissue injury.

References and Notes

1. V. A. Fadok *et al.*, *J. Clin. Invest.* **101**, 890 (1998).
2. J. S. Munger *et al.*, *Cell* **96**, 319 (1999).
3. A. Aruffo, I. Stamenkovic, M. Melnick, C. B. Underhill, B. Seed, *Cell* **61**, 1303 (1990).
4. A. Bartolazzi, R. Peach, A. Aruffo, I. Stamenkovic, *J. Exp. Med.* **180**, 53 (1994).
5. Q. Yu, B. P. Toole, I. Stamenkovic, *J. Exp. Med.* **186**, 1985 (1997).
6. H. C. DeGrendele, P. Estess, M. H. Siegelman, *Science* **278**, 672 (1997).
7. T. C. Laurent, J. R. Fraser, *FASEB J.* **6**, 2397 (1992).
8. C. M. McKee *et al.*, *J. Clin. Invest.* **98**, 2403 (1996).
9. R. Schmits *et al.*, *Blood* **90**, 2217 (1997).
10. I. Y. R. Adamson, H. B. Drummond, *Am. J. Pathol.* **77**, 185 (1974).
11. C. B. Underhill, H. A. Nguyen, M. Shizari, M. Culty, *Dev. Biol.* **155**, 324 (1993).
12. M. M. Guo, J. E. Hildreth, *Anal. Biochem.* **233**, 216 (1996).
13. J. D. McNeil, O. W. Wiebkin, W. H. Betts, L. G. Cleland, *Ann. Rheum. Dis.* **44**, 780 (1985).
14. L. Roden *et al.*, *Ciba Found. Symp.* **143**, 60 (1989).
15. P. M. Sampson, C. L. Rochester, B. Freundlich, J. A. Elias, *J. Clin. Invest.* **90**, 1492 (1992).
16. H. G. Lee, M. K. Cowman, *Anal. Biochem.* **219**, 278 (1994).
17. S. P. Hart, G. J. Dougherty, C. Haslett, I. Dransfield, *J. Immunol.* **159**, 919 (1997).
18. Apoptotic cells were detected in paraffin-embedded sections with DeadEnd Colorimetric Apoptosis Detection System (Promega, Madison, WI) following manufacturer's instructions.
19. C. Haslett, L. A. Guthrie, M. M. Kopaniak, R. B. J. Johnston, P. M. Henson, *Am. J. Pathol.* **119**, 101 (1985), and (*2*).
20. Q. Yu, I. Stamenkovic, *Genes Dev.* **14**, 163 (2000).
21. Samples were analyzed with TGF-β_1 E_{max} Immuno-Assay System (Promega, Madison, WI) following manufacturer's instructions.
22. Six- to eight-week-old mice were irradiated with 1000 rads (^{137}Cs radiator) followed by intravenous injection of 5 million bone marrow cells.
23. H. C. DeGrendele, M. Kosfiszer, P. Estess, M. H. Siegelman, *J. Immunol.* **159**, 2549 (1997).
24. A. Q. Rafi-Janajreh *et al.*, *J. Immunol.* **163**, 1619.

25. Supported by a grant from the National Heart Lung and Blood Institute HL60539 (P.W.N.). P.T. was supported by the Swedish Heart Lung Foundation.

9 January 2002; accepted 4 March 2002

Subnuclear Compartmentalization of Immunoglobulin Loci During Lymphocyte Development

Steven T. Kosak,[1]* Jane A. Skok,[3] Kay L. Medina,[1] Roy Riblet,[4] Michelle M. Le Beau,[2] Amanda G. Fisher,[3] Harinder Singh[1]†

Immunoglobulin (Ig) loci are selectively activated for transcription and rearrangement during B lymphocyte development. Using fluorescence in situ hybridization, we show that Ig heavy (H) and Igκ loci are preferentially positioned at the nuclear periphery in hematopoietic progenitors and pro-T cells but are centrally configured in pro-B nuclei. The inactive loci at the periphery do not associate with centromeric heterochromatin. Upon localization away from the nuclear periphery in pro-B cells, the IgH locus appears to undergo large-scale compaction. We suggest that subnuclear positioning represents a novel means of regulating transcription and recombination of IgH and Igκ loci during lymphocyte development.

Constitutive heterochromatin and the nuclear periphery are the two major classes of transcriptionally repressive nuclear subcompartments. Evidence from studies in *Drosophila* and mammals suggests that the organization of genes into heterochromatin may be one mechanism of regulated transcriptional repression (*1–4*). The role of the nuclear periphery as a repressive compartment has been well established in *Saccharomyces cerevi-*

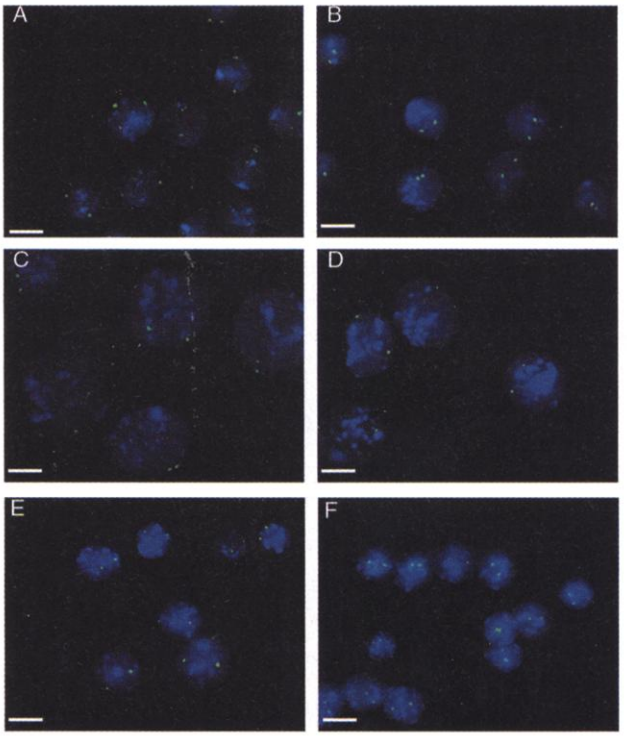

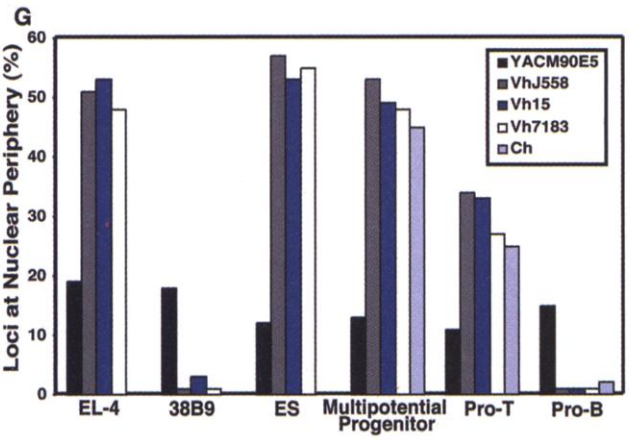

Fig. 1. IgH loci are enriched at the nuclear periphery in non-B lineage cells. 2D FISH analysis was performed with bacterial artificial chromosome (BAC) probes [VhJ558 (526A21), Vh15 (243G9), Vh7183 (167C1), Ch (34H6)] and a yeast artificial chromosome (YAC) probe (YAC M90E5). The green signals correspond to the VhJ558 probe, and the nuclei were counterstained with DAPI (blue): (**A**) EL-4 T cells; (**B**) 38B9 pro-B cells; (**C**) ES cells; (**D**) multipotential progenitors, bone marrow–derived hematopoietic Lin^- cells; (**E**) pro-T cells, DN thymocytes; and (**F**) pro-B cells generated from multipotential progenitors. Scale bars, 10 μm. (**G**) Signals were scored for peripheral localization by measuring images captured on a Zeiss Axioplan epifluorescence microscope (100× objective) with NIH Image software. Signals located at a radial distance (*R*) of 0.8 or greater in relation to the nuclear periphery (ascertained through the extremity of DAPI staining) were scored as peripheral (*16*). For a given cell type, at least 50 nuclei were scored with each probe.

siae. Yeast telomeres form clusters at the nuclear periphery, which leads to enrichment of Sir proteins that are involved in gene silencing (*1, 5*). In human nuclei, analysis of whole chromosomes has revealed that a gene-poor chromosome is preferentially localized to the nuclear periphery, whereas a gene-rich chromosome is more centrally disposed (*6*). However, it remains to be determined whether gene activity in higher eukaryotes is regulated by perinuclear localization.

Immunoglobulin heavy (IgH) and light chain (IgL) loci undergo regulated transcription and rearrangement during B lymphocyte development. Ig loci are not substantially recombined in developing T lymphocytes, even though these cells share the recombinase proteins (Rag-1 and Rag-2), which are also used to rearrange T cell receptor (TCR) loci (*7*). The "accessibility hypothesis" suggests that developmentally programmed V(D)J recombination is controlled by localized alterations in chromatin structure (*8–13*). Whether such a mechanism is sufficient to account for lineage-specific accessibility of Ig loci is currently unknown. Given the evidence that eukaryotic gene activity can be regulated by subnuclear compartmentalization, we investigated whether such a process might play a role in controlling the transcription and rearrangement of Ig loci during B lymphocyte development.

The IgH locus is recombined to produce a functional gene from three groups of gene segments, V, D, and J, which are sequentially activated for germline transcription before their rearrangement. During the pro-B stage of development, the V_H array is transcribed and is poised to undergo V-to-DJ recombination. Two-dimensional (2D) fluorescence in situ hybridization (FISH) analysis was used to examine the nuclear disposition of IgH loci in murine pro-B (38B9) and T (EL-4) cell lines (*14*). Germline V_H gene segments (VhJ558) are transcriptionally active in 38B9 but not EL-4 cells (*15*). Strikingly, about 50% of signals from each of three V_H probes (VhJ558, Vh15, and Vh7183) were preferentially localized to the nuclear periphery ($R \geq 0.8$) (*16*) in EL-4 cells (Fig. 1, A and G). However, in 38B9 nuclei the IgH loci were centrally disposed ($R < 0.8$), often with both alleles in close proximity (Fig. 1, B and G). If the IgH loci were randomly distributed in the nucleus, then a theoretical maximum of 22% of the FISH signals would be expected to be peripheral in this analysis (*14*). To verify our 2D results, we performed three-dimensional (3D) FISH. Confocal analysis showed 95% of the VhJ558 signals at the periphery in EL-4 nuclei; however, only 5% were perinuclear in 38B9 cells (Fig. 2, A and B) (*14, 17*). These data validate our 2D approach and confirm that the IgH locus is enriched at the nuclear periphery in EL-4 T cells, whereas it is excluded from this domain in 38B9 pro-B nuclei.

To determine whether the subnuclear compartmentalization of the IgH locus is modulated during lymphocyte development, we performed 2D FISH analysis on multipotential hematopoietic progenitors (Lin^-), pro-B cells generated from these multipotential progenitors, and pro-T cells (DN thymocytes) (*14*). The pro-B cells carried D-J rearranged IgH alleles and expressed germline VhJ558 gene transcripts that were not detected in the multipotential progenitors and pro-T cells (*15*). About 50% of the V_H signals in multipotential progenitors and 30% in pro-T cells were localized to the nuclear periphery (Fig. 1, D, E, and G). In contrast, fewer than 5% of V_H signals were peripheral in pro-B nuclei (Fig. 1, F and G). The reduced degree of perinuclear localization in pro-T cells is correlated with their ability to undergo limited D_H-J_H rearrangement (*7*).

A C_H probe that lies at the 3′ end of the IgH locus consistently showed a lower percentage of peripheral signals in multipotential progenitors and pro-T cells compared with the 5′ VhJ558 probe (Fig. 1G). This raises the possibility that the 3-Mb IgH locus may be selectively associated with

[1]Department of Molecular Genetics and Cell Biology, Howard Hughes Medical Institute, [2]Department of Medicine, University of Chicago, Chicago, IL 60637, USA. [3]Lymphocyte Development Group, MRC Clinical Sciences Centre, Imperial College School of Medicine, Hammersmith Hospital, London W12 0NN, UK. [4]Torrey Pines Institute for Molecular Studies, San Diego, CA 92121, USA.

*Present address: Division of Basic Sciences, Fred Hutchinson Cancer Research Center, 1100 Fairview Avenue North, Seattle, WA 98109, USA.

†To whom correspondence should be addressed. E-mail: hsingh@midway.uchicago.edu

the nuclear periphery through the distal V gene segments, which may not preclude accessibility of the proximal D-J region to transcription and recombination factors. Note that a control probe (YAC M90E5) located about 8 cM from the IgH locus did not vary in its distribution pattern in the different cell types (Fig. 1G). The compartmentalization of inactive IgH loci at the nuclear periphery appears to represent the default state. Consistent with this possibility, IgH loci are found to be perinuclear in embryonic stem (ES) cells (Fig. 1, C and G). These results demonstrate that the subnuclear positioning of the IgH locus is regulated during lymphocyte development.

It has been shown that a subset of centromeric heterochromatin clusters localize to the nuclear periphery (*18*). To test whether the peripheral location of the IgH locus may be due to its association with such a heterochromatin domain, we performed 3D FISH with the VhJ558 probe and a probe to γ-satellite DNA, the major repetitive element of mouse

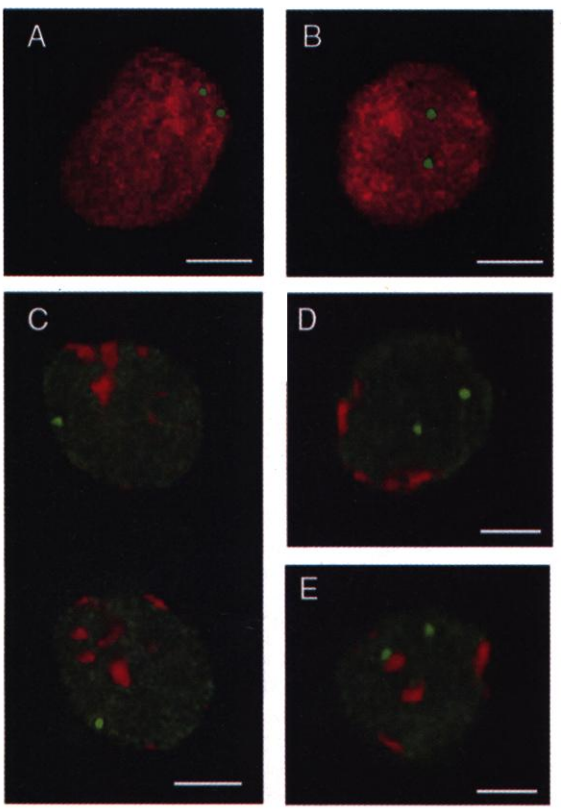

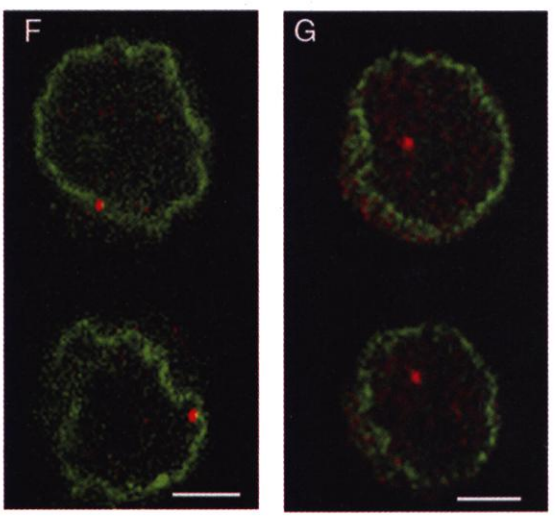

Fig. 2. The peripheral location of the IgH locus in EL-4 nuclei is not due to association with centromeric heterochromatin. Images shown are single confocal optical sections through EL-4 T cells (**A**, **C**, and **F**) and 38B9 pro-B cells (**B**, **D**, **E**, and **G**). Scale bars, 2 μm. (A and B) 3D FISH analysis with the VhJ558 probe (green) in which nuclei were counterstained with propidium iodide (red). (C to E) Dual-color 3D FISH with γ-satellite (red) and VhJ558 (green) probes. In (C), two optical sections showing VhJ558 signals of the same nucleus are indicated; (D) and (E) represent two different nuclei in which both alleles are seen in the same optical plane. In a small proportion of 38B9 nuclei, one IgH signal appeared close to the γ-satellite signal (E). (F and G) Immuno-FISH analysis using antisera to the NH_2- and COOH-terminal portions of lamin B (green) and the VhJ558 probe (red). At least 50 nuclei of both cell types were scored for each analysis.

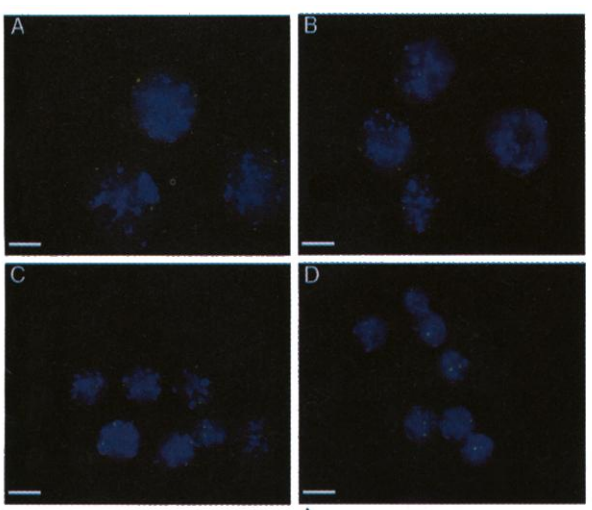

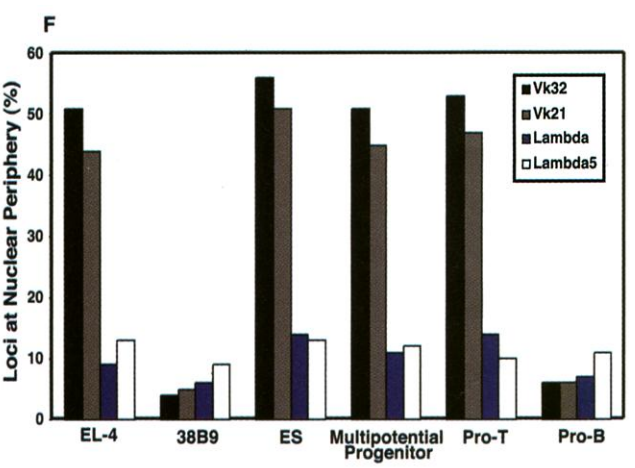

Fig. 3. Subnuclear compartmentalization of Igκ loci, but not Igλ loci, is developmentally modulated. 2D FISH analysis was performed with BAC probes to the Vκ32 (122K2) and Vκ21 (113G24) gene segment families, located at the 5′ and 3′ ends of the Vκ array, respectively. The green signals correspond to the Vκ21 probe, and the nuclei were counterstained with DAPI (blue): (**A**) ES cells, (**B**) multipotential progenitors, (**C**) pro-T cells, and (**D**) pro-B cells (all as described in Fig. 1). Scale bars, 10 μm. (**E**) Reverse transcription polymerase chain reaction analysis using primers that detect β-actin and germline Cκ transcripts (*14*). The Cκ transcripts are induced in 38B9 cells after stimulation with bacterial lipopolysaccharide (10 μg/ml). (**F**) Signals were scored for peripheral localization as described in Fig. 1. This analysis includes probes to the Igλ and λ5 loci. For a given cell type, at least 50 nuclei were scored for each probe.

centromeres (*3*), using EL-4 and 38B9 cells. The IgH loci (97%) in EL-4 nuclei were not associated with centromeric heterochromatin (Fig. 2C). As expected, most of the transcriptionally active IgH loci (89%) in 38B9 nuclei were also not associated with centromeric heterochromatin (Fig. 2, D and E) (*19*). These results demonstrate that IgH loci are not positioned at the periphery by an interaction with centromeric heterochromatin. To examine the possibility that the peripheral IgH loci may be associated with the nuclear lamina, we performed 3D immuno-FISH with the VhJ558 probe and antibodies to the NH_2- and COOH-termini of lamin B, a component of the nuclear lamina (*14, 20*). The analysis showed a predominant juxtaposition of V_H signals (95%) with the nuclear lamina in EL-4 cells (Fig. 2F). Conversely, in 38B9 nuclei, 95% of the V_H signals were positioned away from the nuclear lamina (Fig. 2G). These results raise the possibility that the IgH locus may be sequestered at the nuclear periphery through an interaction with the nuclear lamina or its associated proteins.

We next performed 2D FISH with probes to the Igκ and Igλ light chain loci to investigate whether peripheral localization in non-B lineage cells is a general property of Ig genes. Igκ loci, like their IgH counterparts, were enriched at the nuclear periphery in ES, multipotential progenitor, pro-T, and EL-4 cells but were centrally disposed in pro-B and 38B9 nuclei (Fig. 3, A to D and F). In contrast, Igλ loci did not exhibit an appreciable difference in their localization patterns in the various cell types and were not subject to perinuclear compartmentalization (Fig. 3F). Analysis of another B lineage–specific but non-Ig locus, the λ5 gene, revealed a nuclear distribution pattern similar to the Igλ locus (Fig. 3F). Therefore, the perinuclear positioning of inactive IgH and Igκ loci is not a general property of B lineage–restricted genes.

Interestingly, the unrearranged and centrally positioned Igκ loci are not undergoing appreciable germline transcription in pro-B cells, which suggests that nuclear reconfiguration of Igκ loci precedes germline transcription and is not dependent on it (Fig. 3E). To determine whether recombination is necessary for the nonperipheral nuclear positioning of IgH and Igκ loci, we analyzed pro-B cells expanded from Rag-$2^{-/-}$ bone marrow. The vast majority of the germline loci in these mutant cells were centrally configured (*14*). Therefore, Ig gene recombination is not required for the central localization of the IgH and Igκ loci in pro-B nuclei. The interleukin-7 receptor (IL-7R) is required for B cell development. In its absence, the large majority of B lineage progenitors are arrested at the earliest pro-B stage ($B220^+$, $CD43^+$, $CD19^-$) (*21*). We therefore examined the nuclear disposition of Ig loci in $B220^+$ cells isolated from the bone marrow of IL-$7R\alpha^{-/-}$ mice. Both the IgH and Igκ loci showed enrichment at the nuclear periphery (*14*). As observed for pro-T cells, the frequency of perinuclear localization of IgH loci was reduced relative to Igκ loci and was also correlated with limited D_H-J_H rearrangement (*14, 15*). Therefore, nuclear repositioning of Ig loci is initiated at the early pro-B cell stage. Because IL-7 signaling is implicated in regulating V_H gene accessibility, it remains possible that the IL-7R may function to promote the nuclear reconfiguration of the IgH locus (*22, 23*).

Given the size of the IgH locus (about 3 Mb), we reasoned that two-color FISH analysis with VhJ558/Vh7183 and Vh15/Vh7183 probe pairs could be used to examine its large-scale compaction in relation to its nuclear position. Inactive heterochromatic regions of chromosomes are more compacted than their active euchromatic counterparts (*1*). We therefore expected the inactive IgH loci at the nuclear periphery to appear more compacted than the centrally positioned active loci. However, the opposite correlation was observed, with the IgH probe pairs being more resolvable in EL-4 T cell nuclei (greater

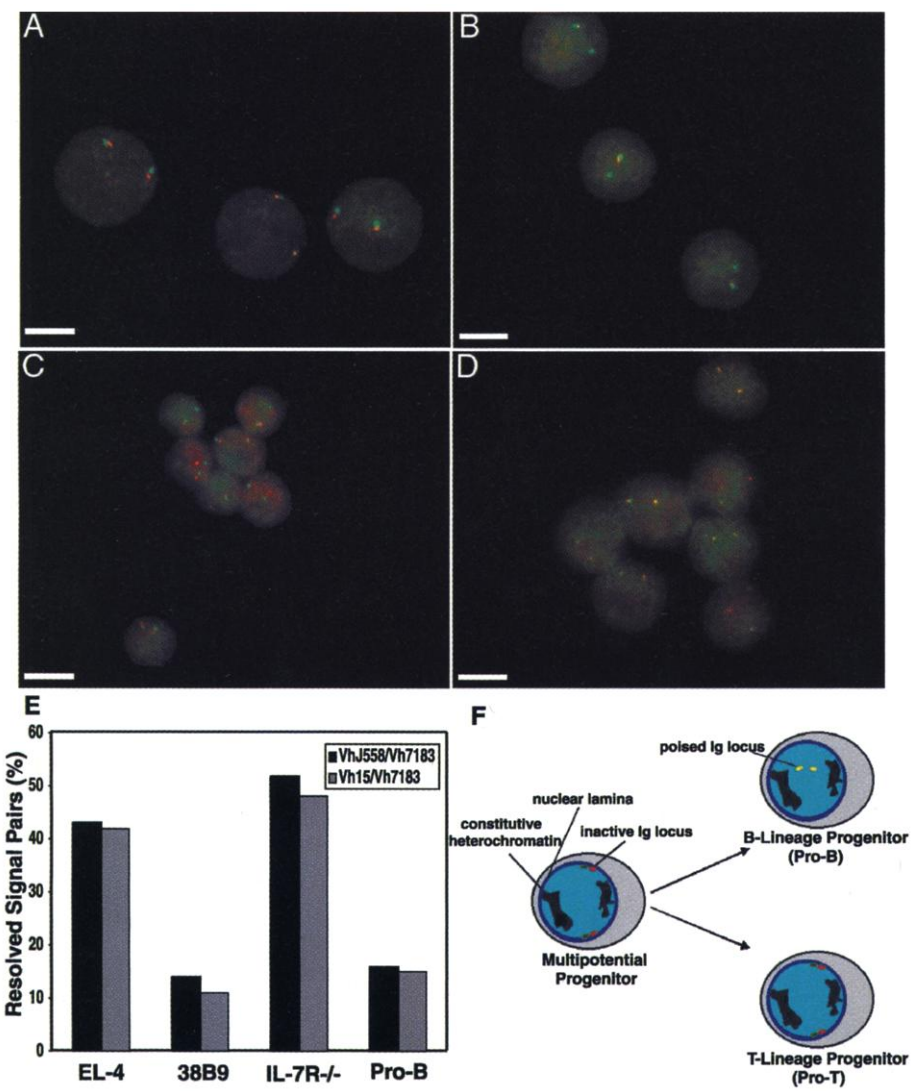

Fig. 4. The IgH locus undergoes large-scale compaction in pro-B cells. Two-color FISH was performed with the VhJ558/Vh7183 and Vh15/Vh7183 probe sets on interphase nuclei: (**A**) EL-4, (**B**) 38B9, and (**C**) $B220^+$ cells from the bone marrow of *IL-7Rα*$^{-/-}$ mice; (**D**) wild-type ex vivo expanded pro-B cells. Images represent the VhJ558/Vh7183 probe set, with the VhJ558 signal in green and the Vh7183 signal in red; DAPI counterstain is omitted so both signals can be seen. Scale bars, 10 μm. (**E**) Percentages of resolved (nonoverlapping) signal pairs. About 100 loci were scored for each cell type for each probe pair. (**F**) A model depicting the developmentally regulated subnuclear compartmentalization of Ig loci. In their default state, the IgH and Igκ loci are sequestered at the periphery through a proposed interaction with the nuclear lamina. During early B cell development, this interaction is disrupted, allowing the two loci to be poised for activation of transcription and V(D)J recombination, which is accompanied by a compaction of the locus.

than 40%) than in 38B9 pro-B nuclei (about 10%) (Fig. 4, A, B, and E) (*14, 16*). Further analysis of pro-B cells and thymocytes verified this lineage-specific difference in compaction (Fig. 4, D and E) (*15*). This differential compaction of the IgH locus was observed in interphase but not metaphase chromosomes. These results raised the possibility that the compacted state of the IgH locus in pro-B nuclei reflects a chromosomal structure that functions to promote long-range V-to-DJ rearrangement. We therefore tested whether the compaction is dependent on the expression of Rag-2 or IL-7R. No appreciable effect on the compacted state was observed in Rag-$2^{-/-}$ pro-B cells (*15*). In contrast, $B220^{+}$ cells isolated from IL-$7R^{-/-}$ bone marrow exhibited a high proportion of resolved signals (about 50%) for both probe pairs, similar to T lineage cells (Fig. 4, C and E). Thus, in the absence of IL-7R expression, the IgH locus does not make a transition into the more compacted state (observed in wild-type pro-B cells) that may facilitate long-range V-to-DJ rearrangement.

Emerging evidence indicates that the nuclear lamina, with its ability to interact directly and indirectly with DNA and chromatin, is important for the functional organization of the nucleus (*24*). We suggest a model in which IgH and Igκ loci, in their default state, are localized at the nuclear periphery through an interaction with the nuclear lamina, which would need to be disrupted during early B lymphocyte development (Fig. 4F). The unique perinuclear localization of the inactive IgH and Igκ loci may be due to their similar genomic structures. Whereas the murine Igλ locus is composed of only three functional V gene segments, the IgH and Igκ loci contain 100 to 200 segments and 140 segments, respectively, and they are both long gene arrays representing about 3 Mb of DNA (*14*). We propose that the positioning of these loci at the periphery inhibits their transcription and rearrangement by sequestration away from the transcription and recombination apparatus and/or by the assembly of a refractory structure. After the loci are released from the nuclear periphery, we suggest that they undergo large-scale compaction whose function may be to facilitate long-range V(D)J rearrangement. It will be interesting to determine whether TCR loci exhibit a reciprocal pattern of lineage-specific subnuclear compartmentalization during lymphocyte development. In any case, the Ig loci represent a model system for probing the means by which the nuclear periphery regulates gene activity in higher eukaryotes.

References and Notes

1. M. Cockell, S. M. Gasser, *Curr. Opin. Genet. Dev.* **9**, 199 (1999).
2. A. K. Csink, S. Henikoff, *Nature* **381**, 529 (1996).
3. K. E. Brown *et al.*, *Cell* **91**, 845 (1997).
4. C. Francastel *et al.*, *Cell* **99**, 259 (1999).
5. E. D. Andrulis, A. M. Neiman, D. C. Zappulla, R. Sternglanz, *Nature* **394**, 592 (1998).
6. J. A. Croft *et al.*, *J. Cell Biol.* **145**, 1119 (1999).
7. D. G. Schatz, M. A. Oettinger, M. S. Schlissel, *Annu. Rev. Immunol.* **10**, 359 (1992).
8. G. D. Yancopoulos, F. W. Alt, *Cell* **40**, 271 (1985).
9. P. Stanhope-Baker, K. M. Hudson, A. L. Shaffer, A. Constantinescu, M. S. Schlissel, *Cell* **85**, 887 (1996).
10. F. McBlane, J. Boyes, *Curr. Biol.* **10**, 483 (2000).
11. M. T. McMurry, M. S. Krangel, *Science* **287**, 495 (2000).
12. D. B. Roth, S. Y. Roth, *Cell* **103**, 699 (2000).
13. B. P. Sleckman, J. R. Gorman, F. W. Alt, *Annu. Rev. Immunol.* **14**, 459 (1996).
14. Supplementary figures and details of experimental procedures are available on *Science* Online at www.sciencemag.org/cgi/content/full/296/5565/158/DC1.
15. S. T. Kosak, H. Singh, unpublished data.
16. Captured images were scored for nuclear localization of the relevant signals with NIH Image software, with the extremity of 4′,6′-diamidino-2-phenylindole (DAPI) staining representing the perimeter of the nucleus. The center of each nucleus was determined by measuring intersecting diameters. From the center, a radial measurement was made through the signal to the perimeter, and the distance from the center to the signal was then determined. The radial fraction (*R*), the ratio of distance to signal/distance to perimeter, represents the position of the signal (or locus) in the nucleus. For example, an *R* of 1 indicates the coincidence of the signal with the nuclear perimeter. We chose an *R* value of 0.8 to 1.0 to represent a peripheral signal, permitting a directed analysis of the difference in localization in an outer shell of the nucleus. Analysis of compaction of the IgH locus was achieved by overlaying independent images for each probe and DAPI in Adobe Photoshop. A resolvable probe pair was defined as one in which the signals were completely distinct (i.e., showed no overlap).
17. 3D FISH was performed as described (*3*); samples were treated to preserve their 3D nuclear structure (*15*). Cells were analyzed with a Leica NT-SP2 confocal system. For 3D analysis of subnuclear localization, stacked optical sections were viewed as a 3D image, which was rotated at 60° angles to determine the proximity of the VhJ558 signal to the extremity of the nucleus (as visualized by propidium iodide staining). Those signals that were either coincident or directly juxtaposed to the propidium iodide–defined border were scored as being at the nuclear periphery. For dual-color 3D FISH, loci were scored as associated with centromeric heterochromatin when locus-specific and γ-satellite signals showed overlap.
18. D. E. Comings, *Hum. Genet.* **53**, 131 (1980).
19. J. A. Skok *et al.*, *Nature Immunol.* **2**, 848 (2001).
20. Immuno-FISH was performed as described (*3, 15*). Cells were analyzed with a Leica NT-SP2 confocal system. Optical Z-sections were collected at 0.2-μm steps through each nucleus. Association was scored when a locus-specific signal showed overlap with lamin B staining.
21. J. J. Peschon *et al.*, *J. Exp. Med.* **180**, 1955 (1994).
22. A. E. Corcoran, A. Riddell, D. Krooshoop, A. R. Venkitaraman, *Nature* **391**, 904 (1998).
23. D. Chowdhury, R. Sen, *EMBO J.* **20**, 6394 (2001).
24. J. Gotzmann, R. Foisner, *Crit. Rev. Euk. Gene Expr.* **9**, 257 (1999).

25. We thank E. Smith, J. Soderholm, C. Schildkraut, J. Zhou, and J. Woodlawn for useful discussions; N. Dillon for the γ-satellite and λ5 probes; C. Schildkraut for the Igκ probes; and U. Storb for the Igλ probe. Supported by NIH Molecular and Cellular Biology training grant 5T32GM07183 and a travel award from the Burroughs Wellcome Fund (S.T.K.), the Wellcome Trust (J.A.S.), the UK Medical Research Council (A.G.F.), and the Howard Hughes Medical Institute (H.S.).

7 December 2001; accepted 4 March 2002